Acta Geologica Sinica (English Edition), 2022, 96(5): 1647–1658

Fluid Inclusion Studies of Ore and Gangue Minerals from the Piaotang Tungsten Deposit, Southern Jiangxi Province, China

WANG Xudong[1, 2, *], NI Pei[2], YUAN Shunda[3], LIU Jiqiang[4], LI Mingyong[1] and LIU Hongxin[1]

[1] *Yuanpei College of Shaoxing University, Shaoxing, Zhejiang 312000, China*
[2] *State Key Laboratory for Mineral Deposit Research, Institute of Geo-Fluids, School of Earth Science and Engineering, Nanjing University, Nanjing 210093, China*
[3] *MLR Key Laboratory of Metallogeny and Mineral Assessment, Institute of Mineral Resources, Chinese Academy of Geological Sciences, Beijing 100037, China*
[4] *Key Laboratory of Submarine Geosciences, Second Institute of Oceanography, Ministry of Natural Resources, Hangzhou 310012, China*

Abstract: The Piaotang deposit is one of the largest vein-type W-polymetallic deposits in southern Jiangxi Province, South China. The coexistence of wolframite and cassiterite is an important feature of the deposit. Based on detailed petrographic observations, microthermometry of fluid inclusions in wolframite, cassiterite and intergrown quartz was undertaken. The inclusions in wolframite were observed by infrared microscope, while those in cassiterite and quartz were observed in visible light. The fluid inclusions in wolframite can be divided into two types: aqueous inclusions with a large vapor-phase proportion and aqueous inclusions with a small vapor-phase ratio. The homogenization temperature (T_h) of inclusions in wolframite with large vapor-phase ratios ranged from 280°C to 390°C, with salinity ranging from 3.1 to 7.2 wt% NaCl eq. In contrast, the T_h values of inclusions with small vapor-phase ratios ranged from 216°C to 264°C, with salinity values ranging from 3.5 to 9.3 wt% NaCl eq. T_h values of primary inclusions in cassiterite ranged from 316°C to 380°C, with salinity ranging from 5.4 to 9.3 wt% NaCl eq. T_h values for primary fluid inclusions in quartz ranged from 162°C to 309°C, with salinity values ranging from 1.2 to 6.7 wt% NaCl eq. The results show that the formation conditions of wolframite, cassiterite and intergrown quartz are not uniform. The evolutionary processes of fluids related to these three kinds of minerals are also significantly different. Intergrown quartz cannot provide the depositional conditions of wolframite and cassiterite. The fluids related to tungsten mineralization for the NaCl-H_2O system had a medium-to-high temperature and low salinity, while the fluids related to tin mineralization for the NaCl-H_2O system had a high temperature and medium-to-low salinity. The results of this study suggest that fluid cooling is the main mechanism for the precipitation of tungsten and tin.

Key words: fluid inclusion, ore mineral, gangue mineral, infrared microscopic study, quartz-vein-type-tungsten deposit, Piaotang

Citation: Wang et al., 2022. Fluid Inclusion Studies of Ore and Gangue Minerals from the Piaotang Tungsten Deposit, Southern Jiangxi Province, China. Acta Geologica Sinica (English Edition), 96(5): 1647–1658. DOI: 10.1111/1755-6724.14900

1 Introduction

The Piaotang quartz-vein-type tungsten deposit is one the largest tungsten deposits in southern Jiangxi Province, as well as one of the tungsten deposits with the largest reserves in this area (Xu et al., 2008). The phenomenon of tin coexisting with tungsten is very common in the Nanling metallogenic belt (Hua et al., 2008) and the Piaotang tungsten deposit is a typical deposit, with these characteristics.

As a famous W-polymetallic deposit, the Piaotang tungsten deposit has been studied since the 1940s (Xu and Ding, 1943; Nan, 1943; Yan, 1944), a great deal of research subsequently being carried out, including analysis of the mineralogy (Zhang, 1960; Chen, 1982), petrogeochemistry and geochronology of diagenesis (Hua et al., 2003; Zhang et al., 2009; He et al., 2010; Bai et al., 2011), metallogenic mechanisms and ore-forming fluids (Mu et al., 1984; Zhang et al., 1984; Wang et al., 2008, 2010, 2013).

Fluid inclusions trapped in minerals represent our most reliable source of information on the temperature, pressure and fluid composition attending a variety of geological processes (Roedder, 1984). As most ore minerals are opaque to visible light, fluid inclusions in transparent gangue minerals, such as quartz, fluorite and carbonates, have commonly been studied in previous research. This study is based on the assumption that the ore minerals and associated gangue minerals are formed under the same conditions. In most cases, contemporaneous deposition cannot be demonstrated by unambiguous textural evidence, even though the gangue and ore minerals are spatially intergrown.

The use of an infrared microscope made it possible to

* Corresponding author. E-mail: wwwggd_009@163.com

© 2022 Geological Society of China

study the fluid inclusions in opaque minerals (Campbell et al., 1984, Campbell and Robinson-Cook, 1987) and this achievement was an important breakthrough in the study of metal deposits. Subsequently, this kind of research was carried out on more metal minerals, including wolframite, enargite, stibnite, pyrite etc. (Giamello et al., 1992; Richards and Kerrich, 1993; Mancano and Campbell, 1995; Lüders, 1996; Lüders and Ziemann, 1999; Lüders et al., 1999; Lüders et al., 2005). Research shows that the examination of primary fluid inclusions in ore minerals is an ideal and reliable method of acquiring accurate information about ore-forming fluids (Bailly et al., 2000; Bailly et al., 2002; Kouzmanov et al., 2002; Lindaas et al., 2002; Hagemann and Lüders, 2003; Kucha and Raith, 2009; Kouzmanov et al., 2010; Wei et al., 2012; Su et al., 2015; Huang et al., 2015).

Wolframite is the dominant ore mineral in the Piaotang W-polymetallic deposit, cassiterite being the subordinate ore mineral in this deposit, as well as one of the few ore minerals suitable for fluid inclusion studies in visible light (Little, 1960; Haapala and Kinnunen, 1979; Campbell and Panter, 1990). The fluid inclusions in quartz and cassiterite have been studied in the Piaotang deposit (Wang et al., 2008, 2013), fluid inclusions in wolframite only having been mentioned in the study of numerous deposits in southern Jiangxi (Ni et al., 2015, 2020). Independent study of fluid inclusions in the wolframite of this deposit was lacking, the comparative study of fluid inclusions in wolframite and cassiterite not having been carried out. As a result, accurate ore-forming fluid information relating to the fluid evolutionary processes had not been obtained. Thus, the fluid inclusions in wolframite, cassiterite and intergrown quartz in the Piaotang tungsten deposit were studied primarily with the objective of: (1) obtaining accurate information about the ore-forming fluids; (2) revealing the similarities and differences in the mineralizing conditions for tungsten and tin in the same deposit; and (3) investigating the mechanism for the formation of this deposit. The fluid inclusion assemblage (FIA) method (Goldstein and Reynolds, 1994; Goldstein, 2003) was utilized in this study, in order to make the data more effective and representative.

2 Geological Setting

The southern Jiangxi region is located in the western area of the Cathaysian Block, which is situated on the internal side of the subduction zone of the Western Pacific plate. The metallogenic belt of this region is located at the intersection of the Wuyishan and Nanling ranges (Zhu et al., 1981). The Sinian–Cambrian strata and the Devonian strata are widely distributed throughout this area, both having tungsten content several to dozens of times higher than the Clark value of the crust (Xu et al., 1984a). The intrusive rocks are mainly granites, accompanied by a small number of intermediate basic rocks. The granites intruded in multiple stages, with the mineralization-related granites showing evidence of high-silica, alkali-rich, volatile-rich and aluminum supersaturation, which can be regarded as a classical type of transformation-type granite (Xu et al., 1984b). The ore resources of the southern Jiangxi region are quite rich and are especially well-known for their high production of tungsten.

The Piaotang tungsten deposit is a large-scale quartz vein-type tungsten polymetallic deposit in this area, mainly containing wolframite and cassiterite, with lesser amounts of molybdenite, bismuthite, chalcopyrite, sphalerite, galena, etc. The exposed strata of this region are mainly from the middle-upper Cambrian metamorphic series, which is composed of low-grade metamorphic sandstone and slate, as well as a small amount of siliceous slate with sporadically distributed Devonian sandy gravel.

In the study area, the tectonic movements are multi-cycled. A strong fold formed in the Caledonian period is a closed extrusion multiple syncline. The axial direction of the fold is NNE, with the axial plane inclined to the SE, the inclination angle varying between 60° and 70°. Faults developed during the Yanshanian, mainly being composed of apparent EW-trending compressive faults and NE-trending compressive-shear faults. The connecting points of faults control the peaks of Yanshanian concealed granite and provide favorable space conditions for ore-bearing quartz veins.

The Hercynian quartz diorite exposed in the mining area has a single grain zircon U-Pb age of 439 ± 2 Ma (He et al., 2010). The quartz diorite is controlled by the NE-trending and NW-trending faults, with no contact metamorphism developed. Therefore, the evidence precludes a genetic relationship between the intrusion and the mineralization. Tumor-like Yanshanian medium-fine grained porphyritic biotite granite is concealed at an elevation below 300 m, with a single grain zircon U-Pb age of 158 ± 3 Ma (He et al., 2010). Biotite granite is controlled by the NE-trending and EW-trending faults. The boundary between intrusive body and wall rock is clear where contact metamorphism developed. Hornfelsization is widely distributed in the wall rocks (Fig. 1).

The Piaotang tungsten deposit is composed of hundreds of ore-bearing quartz veins, which are densely distributed in the wall rock and extend downwards into the intrusive body. The elevations of the ore-bearing quartz veins generally range from 200 to 750 m, while the lengths of these veins range from 100 to 1200 m. The widths of the veins can be anywhere from a few centimeters to 2 meters. The trend of ore-bearing quartz veins is nearly east-westward, inclining to the north with angles of 75° to 82°. The ore bodies are further divided into veinlet belt-type and individual thick vein-type, the veinlet belt-type being the main type of the deposit. As a whole, the deposit displays veinlet belts in its upper part and transitions to individual thick veins downwards, with the typical ‘five-story building’ model (No. 932 Team of Nonferrous Metals Geological Exploration Company of Guangdong Province, 1966).

Greisenization is usually developed on both sides of the veins. The mineralization of the quartz veins took place over multiple epochs and stages. According to the cross-cutting relationships between veins, mineral assemblages, ore textures and structures, as well as the type of alteration, Shan (1976) divided the mineralization of the

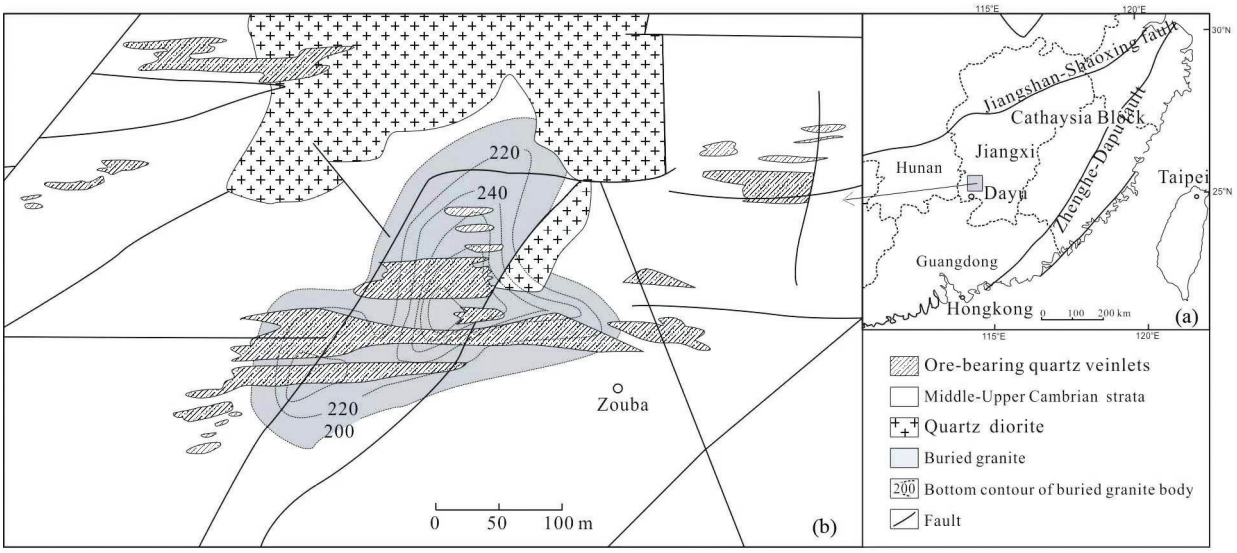


Fig. 1. Geological sketch of the Piaotang tungsten deposit (after Shan, 1976).

Piaotang tungsten deposit into six stages, corresponding to six types of veins. The veins from the (beryl)-cassiterite-wolframite-quartz stage have the most important industrial value of all these types. The mica $^{40}Ar/^{39}Ar$ age of the ore-bearing quartz veins is 152 ± 1.9 Ma (Zhang et al., 2009), which is slightly younger than the emplacement age of the granite. The minerals of the ore-bearing quartz veins include quartz and wolframite, cassiterite, sulfides, carbonates, etc. The major ore texture includes euhedral crystal texture, with minor metasomatic textures and cataclastic textures being observed. The major ore structures include massive structure, disseminated structure, comb-like structure, banded structure, brecciated structure and a small number of miarolitic structures.

3 Materials and Methods

A total of 30 samples were collected for fluid inclusion observation and analysis. The veins of the (beryl)-cassiterite-wolframite-quartz mineralization stage (the major mineralization stage) were sampled at 388 m, 448 m and 496 m depth in the Piaotang deposit. The quartz is massive, gray and occasionally milky. Wolframite in the quartz veins is tabular, columnar or needle-like (as shown in Fig. 2a). Cassiterite exhibits subhedral to allotriomorphic texture and occurs symmetrically near the margin of the vein, with colors varying from chocolate brown to dark brown (as shown in Fig. 2b).

The transparency of minerals under infrared microscopy is variable and depends on the changes of major and trace elements (Robinson-Cook et al., 1986). For wolframite, iron content is one of the main factors affecting its transparency under infrared light, as higher iron content results in poorer transparency. However, the transparency of wolframite can be improved by reducing the thickness of the doubly-polished thin-sections. If transparency was not excellent, the thin-sections were polished thinner in order to increase the transparency. Therefore, the thickness of the sections used in this study were about 80–120 μm for wolframite and about 300 μm for cassiterite and quartz, respectively.

Campbell and Panter (1990) selected several minerals that are transparent in infrared and visible light sources, and the measurements of homogenization temperature (Th) and melting temperature (Tm) were compared for individual inclusions. Although several of the Tm values deviated from the 1:1 line, a fairly good correlation of the Th and Tm values of most samples was found between both light sources. In this study, the melting points of pure water inclusions (0°C), pure CO_2 inclusions (−56.6°C), and potassium bichromate (398°C) were measured, under both visible and infrared light. The results indicated that there was no systematic error.

Moreover, infrared microthermometry of opaque minerals revealed that the acquired temperatures of phase transition depend on the infrared light intensity, as internal heating caused by infrared radiation on the Tm and Th of fluid inclusions in opaque minerals will change the interpretation of the fluids and physical-chemical processes involved during ore formation (Moritz, 2006). In order to minimize that influence within this study, the minimum light intensity required was used, based on the premise that the inclusions in wolframite are clear enough. In addition, the position of the measured inclusion was moved away from the center of the field of view of the microscope during the procedure, although it should be noted that this approach certainly decreased the number of inclusions available for measurement.

All fluid inclusion experiments were performed at the State Key Laboratory for Mineral Deposit Research, Nanjing University. The microthermometric measurements of the fluid inclusions were performed using a Linkam THMS 600 heating-freezing stage (temperature range: −195°C to +600°C) mounted on an Olympus BH51 infrared microscope. The stage was calibrated using standard Syn Flinc fluid inclusions, the accuracy of the measured temperatures being found to be about ±0.2°C during cooling and about ±2°C between 100°C and 600°C. Temperatures of phase transitions were observed at a heating rate of 0.1 °C/min. In this study, the fluid inclusions in wolframite,

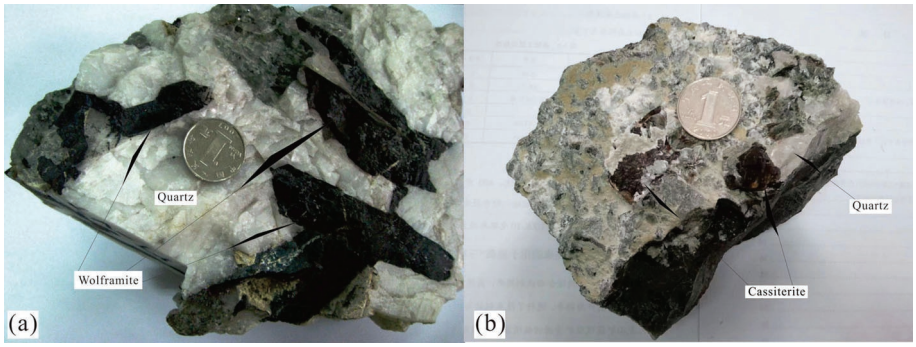


Fig. 2. Cassiterite-wolframite-(beryl)-bearing quartz vein sample from the Piaotang tungsten deposit.

cassiterite and quartz were studied with the same system and the infrared microscope, after having removed the infrared polarizer and analyzer. Freezing tests were performed prior to the heating tests. The reproducibility of Tm and Th measurements was good.

The compositions of inclusions in quartz and cassiterite were analyzed on a Renishaw RM2000 Raman microprobe, using an Ar ion laser with a surface power of 5 mW for radiation excitation (514.5 nm). The detector change-coupled device (CCD) area was 20. In addition, the scanning range of spectra was set between 200 and 3800 cm^{-1}, with an accumulation time of 30 s for each scan.

4 Fluid Inclusion Study

4.1 Fluid inclusion assemblage (FIA)

The petrography and microthermometry of the inclusions in this study were based on the principle of the Fluid Inclusion Assemblage (FIA) (Diamond, 1990; Goldstein and Reynolds, 1994; Goldstein, 2003). A FIA is a group of fluid inclusions that were all trapped at the same time (Goldstein and Reynolds, 1994). FIA is a means of confirming that the inclusions do adhere to 'Roedder's Rules', making the test data more effective and representative (Chi and Lu, 2008). In this study, primary inclusions occurring in small groups with similar vapor/liquid ratios, as well as secondary inclusions along the same healing fissure, were classified as a FIA. If the temperature and salinity of fluid inclusions in the same FIA were uniform, their mean value was taken. If their values were strongly divergent, the effects of later reconstruction were considered, such as necking down, stretching, leaks, or heterogeneous capture (e.g., immiscibility).

4.2 Fluid inclusion petrography

Four types of inclusions were found in quartz, but only one in wolframite and cassiterite.

4.2.1 Quartz

Fluid inclusions in quartz were classified as type I, type II, type III and type IV. In this study, type I fluid inclusions occurring in the same FIA with type III and type IV were not found, type II, type III and type IV only being found in quartz intergrown with wolframite.

Type I fluid inclusions were two-phase liquid-rich aqueous inclusions at about 20°C. This type was the most abundant fluid inclusion in quartz and the primary inclusions (Ia) occurred in small groups (Fig. 3a) or in isolation (Fig. 3b), whereas the secondary inclusions (Ib) were arranged along the healed cracks that cut the boundary of the quartz grain (Fig. 3c).

Type Ia inclusions were generally 5 μm to 10 μm in length, some even exceeding 50 μm. They exhibited ellipsoidal, irregular, elongated, rounded, rectangular or negative crystal shapes. The vapor-phase accounted for between 5 and 15 percent of the total volume in the inclusions. In this study, type Ia inclusions in quartz intergrown with wolframite were named type Ia1, type Ia inclusions in quartz intergrown with cassiterite being referred to as type Ia2.

Type Ib inclusions were smaller than type Ia inclusions, usually 2 μm to 5 μm in length with a round or oval shape, the vapor-phase occupying less than 5 percent of the total volume of the inclusions. In this study, type Ib inclusions in quartz intergrown with wolframite were named type Ib1, type Ib inclusions in quartz intergrown with cassiterite being called type Ib2.

Type II fluid inclusions are monophase aqueous inclusions. This type of inclusion was less prevalent, with a size of 5 μm to 10 μm, mostly in an elongated shape and often coexisting with type I inclusions (Fig. 3d). Based on the spatial relationship of type I and type II inclusions, it was speculated that this type of inclusion might be caused by a 'necking down' process.

Type III aqueous inclusions had one solid phase. The solid phase might be a halite crystal, according to its shape. The abundance of this type of inclusion was extremely low and only one such inclusion was found in this study. The size of this type of fluid inclusion was about 15 μm with an irregular shape, coexisting with type I inclusions (Fig. 3e). These inclusions might be formed by nonuniform capture.

Type IV inclusions were three-phase aqueous-carbonic inclusions, which were very rare, as only two inclusions were found in this study. The CO_2 phase occupied roughly 30% and 70% of the total volume in each of the two inclusions. They had ellipsoidal and rounded shapes with sizes of 8 μm and 10 μm (Fig. 3f).

4.2.2 Wolframite

In order to eliminate any ambiguities caused by host

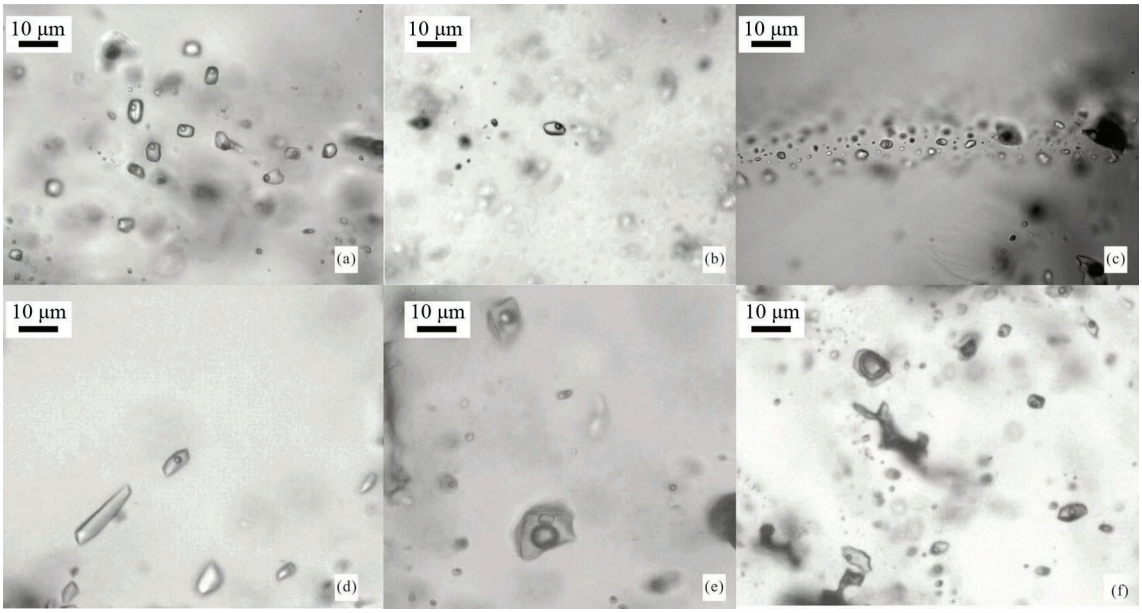


Fig. 3. Fluid inclusions in quartz.

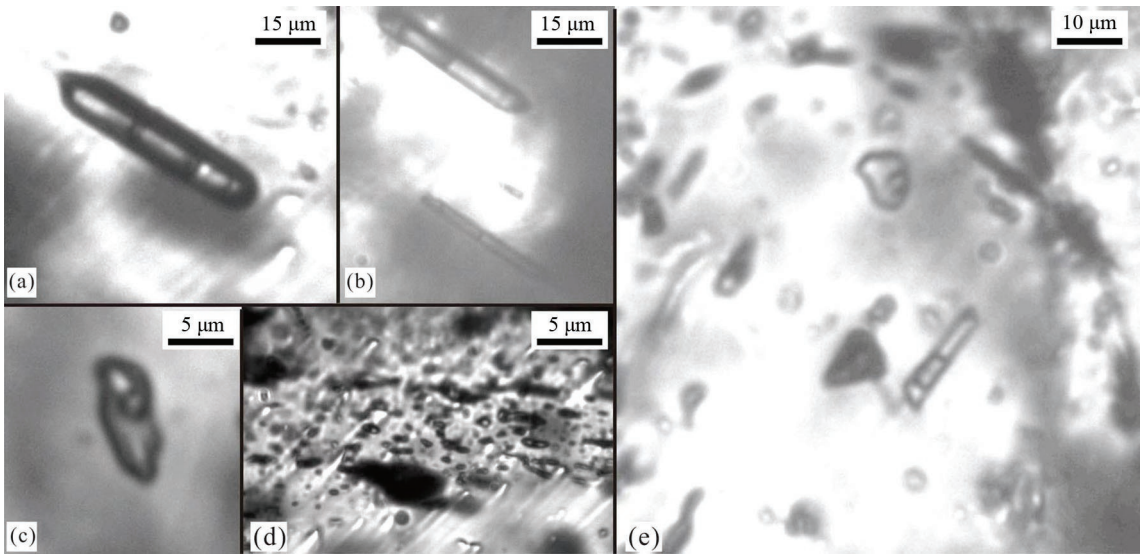


Fig. 4. Fluid inclusions in wolframite.

minerals, type I fluid inclusions in wolframite were denoted as IW. The IW type consisted of two-phase liquid -rich inclusions at about 20°C, further subdivided into inclusions with a higher vapor-phase proportion (IWa type) and a lower vapor-phase ratio (IWb type). Nonuniform transparency of wolframite in infrared light might be caused by compositional variations, which lead to difficulties in distinguishing primary and secondary fluid inclusions. In this study, fluid inclusions along the growth planes and occurring in isolation were regarded as primary fluid inclusions.

The size of IWa type inclusions ranges from 20 μm to 30 μm, although some even exceeded 60 μm. These inclusions mainly exhibited a tubular or needle shape. The vapor-phase accounts for 30 to 40 percent of the total volume, these inclusions being distributed in isolation (Fig. 4a) or along the growth planes (Fig. 4b). The IWb type inclusion can be further subdivided into primary fluid inclusions (IWb1) and secondary fluid inclusions (IWb2). The size of IWb1 type inclusions ranges from 5μm to 10μm, these inclusions having a tubular, elliptical or irregular shape. The vapor-phase accounted for 5 to 15 percent of the total volume, IWb1 inclusions occurring in isolation (Fig. 4c) or in combination with IWa type inclusions (Fig. 4e). The IWb2 type inclusion is smaller than IWa and IWb1 types, most being less than 5μm with a round, oval or irregular shape. The vapor-phase accounted for 5 to 10 percent of the total volume, with distribution along healed cracks (Fig. 4d).

4.2.3 Cassiterite

Type I fluid inclusions in cassiterite are denoted ISn.

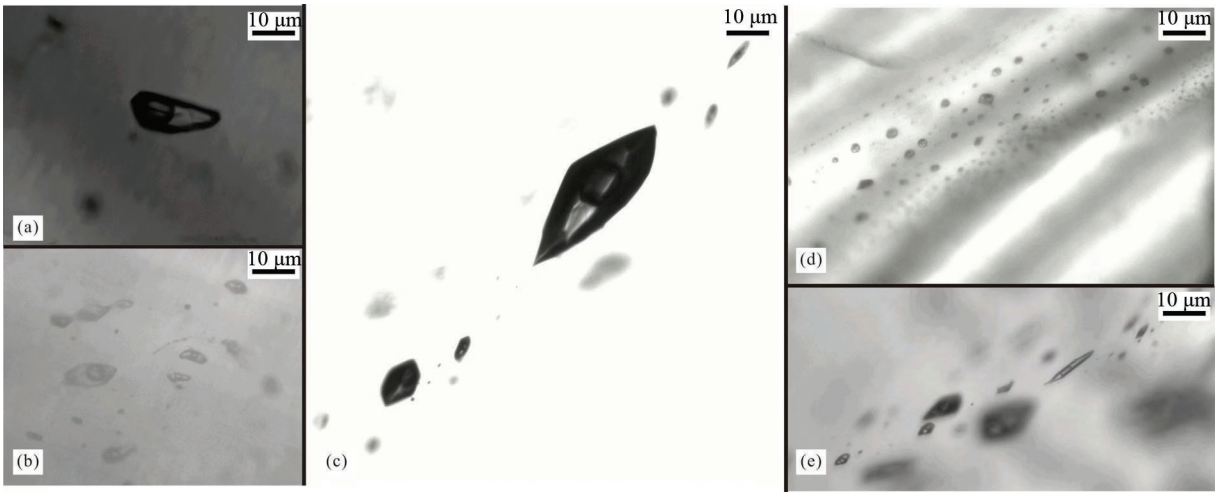


Fig. 5. Fluid inclusions in cassiterite.

The ISn type inclusions were two-phase liquid-rich aqueous inclusions that were generally 5 μm to 20 μm in size, with some exceeding 50 μm. The vapor-phase ranged from 10 to 30 percent of the total volume. Irregular, elliptical, diamond and elongated shapes have been observed for these inclusions, which occur in isolation (Fig. 5a), in small groups (Fig. 5b) or along the growth planes of cassiterite (Fig. 5c, d, e).

4.3 Microthermometry of fluid inclusions

Microthermometrical analyses of inclusions in wolframite, cassiterite and associated quartz were carried out. Freezing was performed prior to heating. Ice was rarely seen directly in the fluid inclusions of wolframite during freezing, although deformations or movements of the vapor bubble, due to freezing and melting of the ice, were often visible. Consequently, when ice was not visible, melting temperatures were obtained by cycling (Goldstein and Reynolds, 1994). Another problem encountered while analyzing inclusions in wolframite is the increase in the opacity of wolframite chips upon heating. This problem was also encountered during homogenization runs of inclusions in wolframite from Panasqueira, Portugal (Campbell et al., 1988). Around 350°C, wolframite becomes remarkably dark, in some cases the sample becoming entirely opaque at about 400°C. This phenomenon can be attributed to the temperature dependence of the infrared absorption edge (Campbell and Panter, 1990). During heating runs in this study, when visibility was lost, the determination of the homogenization temperature was made possible by cycling (Goldstein and Reynolds, 1994). The cycling method for determining the Tm and Th is not as accurate as direct observation of ice or vapor bubble disappearance, but in most cases the reproducibility of the measurements was good.

Microthermometry of fluid inclusions in quartz and cassiterite was based on the experiments of Wang et al. (2008, 2013), with some supplementary work added. Type III and type IV inclusions were not found during microthermometry, due to the quantity being too small. Type II inclusions coexisting with type Ia inclusions might be caused by ‘necking down’ and as this cannot represent the conditions of mineral formation, microthermometry was not carried out for these kind of inclusions in this study. Similarly, given the small size of type Ib1 inclusions in this study, microthermometry was not carried out for these kinds of inclusions either.

Type Ib2 inclusions in quartz coexisting with cassiterite were also measured. During the process of microthermometry, gaseous species, such as CO_2, CH_4 and H_2S, were not found in fluid inclusions in wolframite and cassiterite, indicating that there were no such components in fluid inclusions in wolframite and cassiterite.

The salinity of fluid inclusions in the three kinds of mineral were calculated using the following formula: wt% NaCl eq = 0.00 + 1.78A − 0.0442A2 + 0.000557A3 (Hall et al., 1988). The microthermometric results are listed in Table 1 and plotted in Figs. 6−7.

The results show that the salinity and homogenization temperatures of the fluid inclusions in wolframite, cassiterite and intergrown quartz have obvious differences. In the same mineral, secondary fluid inclusions generally have slightly lower salinity and homogenization temperatures than primary fluid inclusions. However, the salinity of secondary fluid inclusions of wolframite is sometimes higher.

4.4 Laser Raman spectroscopy analyses

Representative fluid inclusions were analyzed by laser Raman spectroscopy. The Raman spectra of type Ia fluid inclusions in quartz coexisting with cassiterite and wolframite displayed a broad water peak, indicating that H_2O was the dominant component of these fluid inclusions (Fig. 8). The results of the Raman spectral analysis are consistent with petrography and microthermometry of this type of fluid inclusion. No valid Raman spectrum could be obtained from fluid inclusions in cassiterite, due to a high level of background interference.

5 Discussion

5.1 Comparison of fluid inclusions in wolframite, cassiterite and intergrown quartz

Based on analysis of fluid inclusions in wolframite,

Table 1 Results of microthermometry of fluid inclusions in ore-bearing quartz veins of major mineralization stages from the Piaotang tungsten deposit

Host mineral	Type	*n*	T_m (°C)	T_h (°C)	Salinity (wt% NaCl eq)	Homogenization way
Quartz coexisting with wolframite	Ia_1	154	−0.7 to −4.5	161–340	1.2–7.2	Liquid
	Ia_2	200	−0.7 to −4.2	162–309	1.2–6.7	Liquid
Quartz coexisting with cassiterite	Ib_2	25	−0.2 to −0.6	168–187	0.4–1.1	Liquid
	I_{Wa}	40	−2.8 to −5.8	280–390	4.6–8.9	Liquid
Wolframite	I_{Wb1}	23	−2.1 to −4.3	216–264	3.5–6.8	Liquid
	I_{Wb2}	8	−2.3 to −4.3	180–187	3.9–6.8	Liquid
Cassiterite	I_{Sn}	75	−3.3 to −6.1	316–380	5.4–9.3	Liquid

Notes: *n* = number of measurements; T_m= melting temperature of ice; T_h = homogenization temperature

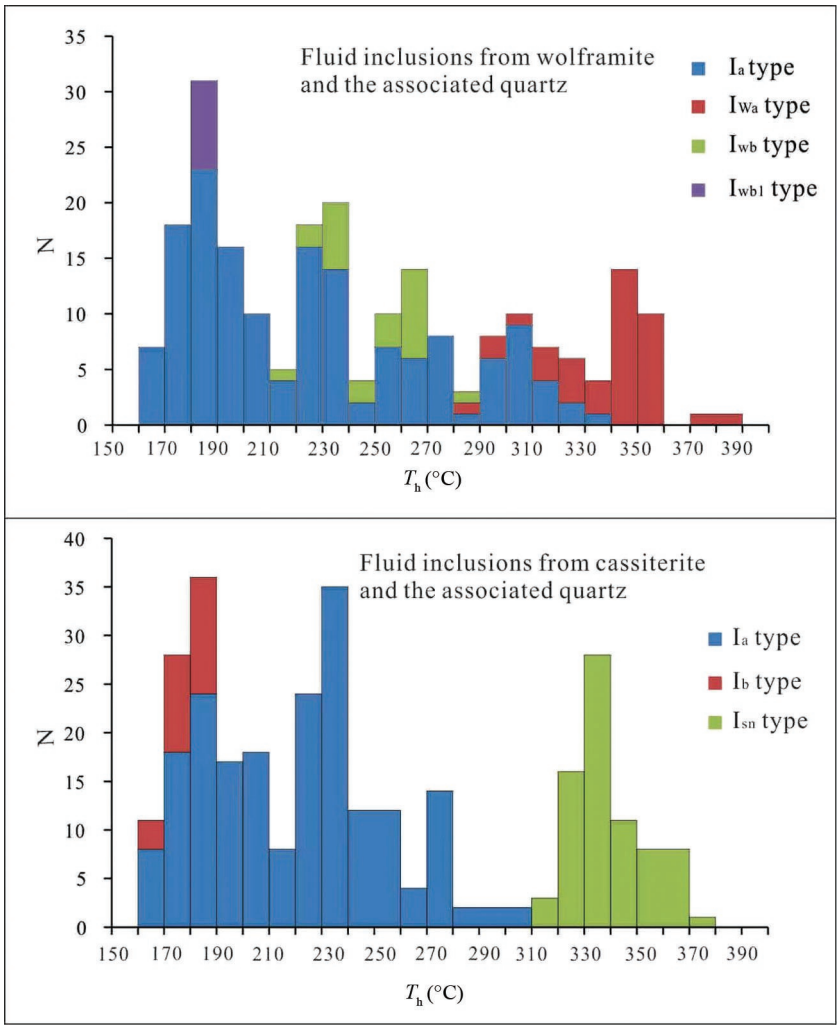


Fig. 6. Histogram of homogenization temperatures of fluid inclusions in wolframite, cassiterite and quartz from the Piaotang deposit.

cassiterite and intergrown quartz, the conclusions can be described as follows: (1) the formation conditions of ore minerals and intergrown gangue minerals are different; (2) the formation conditions of wolframite and cassiterite are clearly different; and (3) there are no significant differences between fluid inclusions in quartz coexisting with cassiterite and those in quartz coexisting with wolframite. The fluid inclusions in cassiterite have higher salinity, considerably higher T_h and a narrower distribution range compared to those in intergrown quartz.

Fluid inclusions in wolframite are more complicated. As noted above, there are two types of fluid inclusions that are differentiated by the percentage volume occupied by the vapor-phase, IWa type and IWb1 type, which are spatially adjacent (Fig. 9). However, the Th and salinity of the IWa type are higher than those of the IWb1 type. The Th of the IWa type inclusions is close to that of the ISn type, whereas its salinity is slightly lower. The Th and salinity of IWb2 type inclusions are consistent with those of type Ia inclusions in coexisting quartz. The differences for Th between inclusions in ore minerals and those in quartz are mainly due to differences in conditions of trapping, rather than being caused by post-reconstruction after the formation of the minerals (Roedder, 1984; Campbell and Panter, 1990). Therefore, primary fluid inclusions in wolframite and cassiterite, rather than quartz,

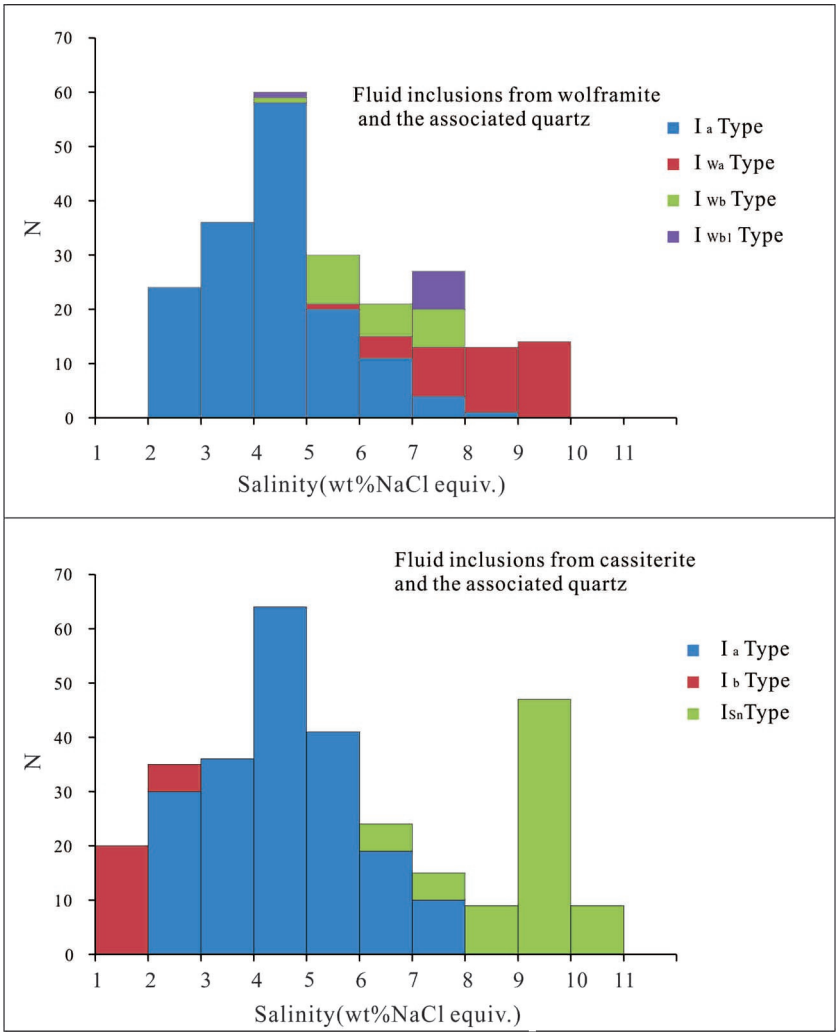


Fig. 7. Histogram of the salinities of fluid inclusions in wolframite, cassiterite and quartz from the Piaotang deposit.

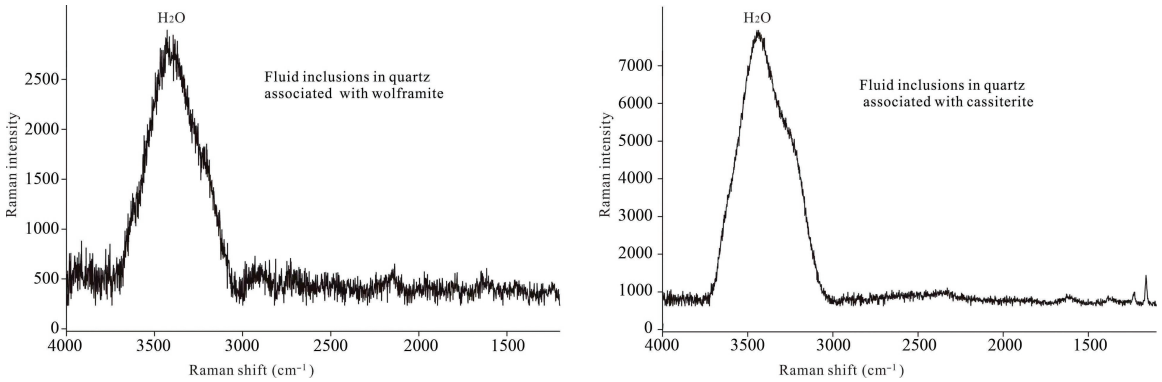


Fig. 8. Raman spectra of fluid inclusions in quartz.

reflect the true formation conditions of tungsten and tin in this deposit.

In this study, no CO_2-bearing fluid inclusions were found in petrographic observations of wolframite or cassiterite. In addition, no phase change related to CH_4, CO_2 or other gaseous species was found by microthermometry. Therefore, fluid inclusions in wolframite and cassiterite do not contain detectable CO_2, CH_4 or other volatiles. Combined with the analysis of fluid inclusions in quartz, the following conclusions can be reached: (1) fluids related to the formation of wolframite are of medium-high temperature and low salinity in the NaCl-H_2O system, with clearly different distribution ranges in homogenization temperature; (2) fluids related to the formation of cassiterite are of high temperature and low salinity in the NaCl-H_2O system; and (3) fluids related

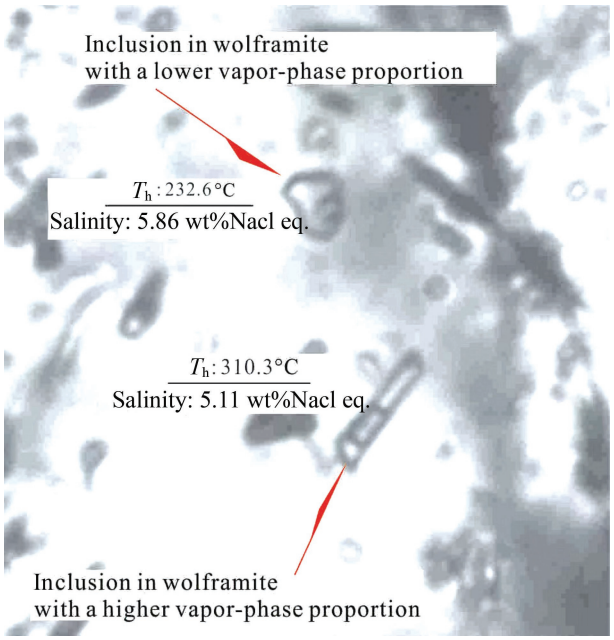


Fig. 9. Two types of fluid inclusions in wolframite.

to the formation of quartz are part of the NaCl-H_2O ± CO_2 system, with larger homogenization temperature variations.

5.2 Evolution of ore-forming fluids

The homogenization temperatures and salinities of fluid inclusions in wolframite and cassiterite lie within a narrow range, with no obvious linear correlation between them (Fig. 10). This characteristic indicates that fluids related to tin and tungsten mineralization may come from a single source, having not experienced any evident mixing process. The obtained values of the Th and salinity of fluid inclusions in wolframite and cassiterite show that the variations in Th are much broader, while the distribution range of salinity is narrow. This further indicates that fluids related to the mineralization of tungsten and tin experienced a cooling process. Furthermore, no vapor-rich fluid inclusions or CO_2-bearing fluid inclusions were found in wolframite or cassiterite. All inclusions were homogenized to a liquid phase, thereby demonstrating that boiling was unlikely to have occurred during ore formation.

The research also shows that the metallogenic process for wolframite is more complex than for cassiterite in the Piaotang deposit. The fluid inclusions with different vapor-phase proportions in wolframite are divided into two obvious distribution ranges, with regards to Th and salinity. The Th and salinity for fluid inclusions with larger vapor proportions are approximate to the values found for inclusions in cassiterite, indicating that some wolframite was formed under similar conditions to cassiterite. The Th and salinity for fluid inclusions in wolframite with a smaller vapor-phase proportion are apparently more like some inclusions in the quartz. This indicates that the precipitation of wolframite was still going on during the formation of quartz, although the crystallization of cassiterite was finished by this time. The differences between the two kinds of fluid inclusions in wolframite show that these two types of inclusions were perhaps captured in different evolutionary processes of the same fluid system. Fluid inclusions with large vapor-phase ratios were more likely to be captured in the initial high temperature environment, while those with small vapor-phase ratios were captured in low temperature environments. Alternatively, at least two hydrothermal events occurred during wolframite formation, these two kinds of fluid inclusions reflecting two diverse hydrothermal activities.

As shown in the diagram of Th versus salinity of fluid inclusions in wolframite, cassiterite and intergrown quartz (Fig. 10), the Th and salinity of Ia type inclusions in quartz show the widest variation, a linear correlation between the Th and salinity being observed. As the fluid temperature went down, salinities also showed a corresponding downward trend, reflecting that the original fluids with a higher salinity and temperature had mixed with cold fluids of lower salinity (Lu et al., 2004). The interfusion of meteoric water during the formation of quartz in this metallogenic stage has also been

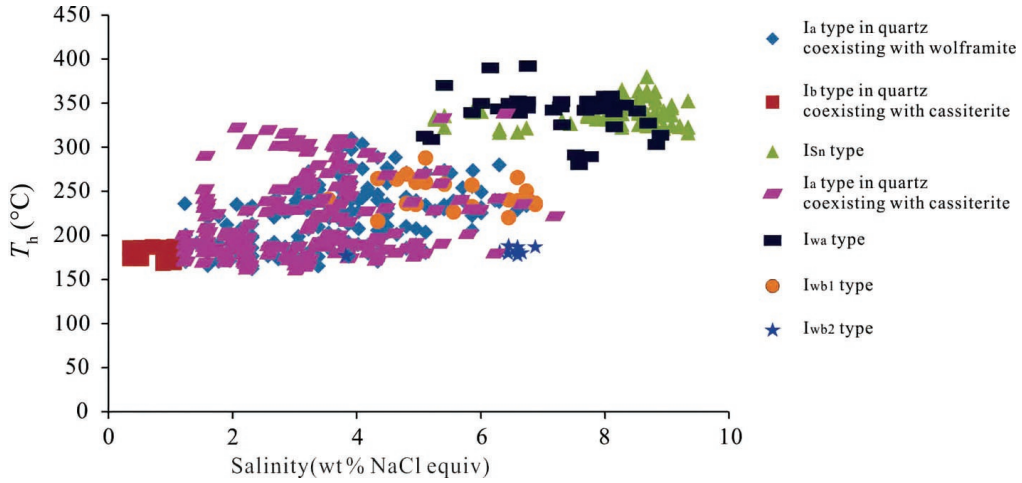


Fig. 10. Diagram of homogenization temperatures versus salinities of aqueous fluid inclusions from the Piaotang deposit.

demonstrated by H-O isotope analysis (Mu et al., 1984; Zhang et al., 1984).

5.3 Precipitation mechanisms for metals in fluids

A considerable number of mechanisms have been proposed to account for mineral deposition in this type of tungsten deposit, including cooling (Ramboz et al., 1985; Seal et al., 1987; Samson, 1990; O'Reilly et al., 1997), fluid mixing (Landis and Rye, 1974; Ramboz et al., 1985; Jackson et al., 1989; Heinrich, 1990; Bailly et al., 2002; Beuchat et al., 2004; Wang et al., 2010), boiling and/or CO_2 effervescence (Higgins and Kerrich, 1982; Ramboz et al., 1982; Seal et al., 1987; Lynch, 1989; Polya, 1989; Giamello et al., 1992; So and Yun, 1994; Graupner et al., 1999; Wang et al., 2010), pH increase associated with water-rock reactions (Kelly and Rye, 1979; Seal et al., 1987; Polya, 1989; Clark et al., 1990; Catallani and Williams-Jones, 1991), pressure decrease (Polya, 1989, 1990) and addition of nonpolar volatiles from wall-rock reactions (O'Reilly et al., 1997). However, most of the above theories are based on characteristics of fluid inclusions in gangue minerals that are intergrown with ore minerals, assuming that gangue minerals and ore minerals formed at the same time, or at least formed under similar conditions and experienced the same or similar evolutionary processes. Studies of fluid inclusions in ore minerals, however, indicate that the conditions suitable for ore minerals to crystallize are quite different from those for the intergrown gangue minerals (Campbell and Robinson-Cook, 1987; Campbell and Panter, 1990). Therefore, it is more reliable to investigate the mechanism of metal precipitation from fluids based on the characteristics of fluid inclusions in the ore minerals.

Boiling fluid inclusion assemblages were not found in either ore minerals or gangue minerals at the major mineralization stage in the Piaotang deposit. The characteristics of the fluid inclusions in quartz indicate that the fluids had undergone a significant fluid mixing process, while the characteristics of fluid inclusions in wolframite indicated that cooling is a key factor for tungsten deposition from fluids, as has also been demonstrated by previous research (Wood and Samson, 2000). In the Piaotang tungsten deposit, the formation of cassiterite is similar to wolframite, so the cooling of the fluid system also acts as the main mechanism for cassiterite crystallization. But that is clearly different from tin, as tungsten has experienced two stages of mineralization.

Based on the results presented in this study, a model for the mineralization of tin and tungsten in the Piaotang deposit is proposed. First, the initial magmatic hydrothermal fluids from the fractional crystallization of granitic magma interacted with crystallographic or sub-solidified rocks, leaching out the ore-forming elements, such as tin and tungsten, which then entered the fissures. Second, the ore-forming fluids underwent a cooling process during cycling and migration, with the declining temperature resulting in reduced solubility of tin and tungsten. In this process, tin and tungsten began to precipitate from the fluid at about 390°C to 380°C and although the precipitation of tin was completed by 320°C, tungsten continued precipitating until 310°C; at this point, quartz began to crystallize and the precipitation of wolframite was interrupted after the temperature decreased to 280°C. Third, the temperature of the ore-forming fluids reduced continuously and mixed with atmospheric water. At this stage, quartz began to precipitate in great abundance, wolframite crystallizing again at about 260°C. The precipitation of tungsten was completed by 210°C, while quartz precipitation continued throughout the fluid's activity.

6 Conclusions

Based on the results of this study, several conclusions are drawn.

(1) The formation conditions of wolframite, cassiterite and coexisting quartz are different. The evolutionary processes of fluids related to mineralization of tungsten and tin are also different. Direct observation and testing of fluid inclusions in ore minerals is the most reliable method of obtaining information on the properties and process of mineralization of ore-forming fluids.

(2) The formation conditions of wolframite and cassiterite are different. The formation of wolframite is more complex, the fluids related to tungsten formation are the NaCl-H_2O fluid system with medium to high temperature and low salinity, as well as a NaCl-H_2O fluid system with high temperature and low salinity for the formation of tin.

(3) The cooling of the fluid system might be the key mechanism that led to the precipitation of tungsten and tin in the fluids.

Acknowledgments

This study was supported by the Science Foundation for Outstanding Young Scholars (41822304) and the Zhejiang Provincial Natural Science Foundation (LZ16D060001). We are sincerely grateful to Dr Yang Xiaonan, Zhou Qing, Li Zhonghai, Wang Yichuan and Gao Qiuzhi who have assisted with language polishing of this manuscript and for important suggestions which helped clarify the ideas expressed in this paper.

Manuscript received Dec. 24, 2020
accepted Dec. 20, 2021
associate EIC: FEI Hongcai
edited by FEI Hongcai

References

Bai, X.J., Wang, M., Lu, K. H., Fang, J.L., Pu, Z.P., and Qiu, H.N., 2011. Direct dating of cassiterite by $^{40}Ar/^{39}Ar$ progressive crushing (in Chinese). Chinese Science Bulletin (Chinese Ver), 56: 1899–1904 (in Chinese with English abstract).

Bailly, L., Bouchot, V., Bény, C., and Milési, J P., 2000. Fluid inclusion study of stibnite using infrared microscopy: An example from the Brouzils antimony deposit (Vendee, Armorican Massif, France). Economic Geology, 95: 221–226.

Bailly, L., Grancea, L., and Kouzmanov, K., 2002. Infrared microthermometry and chemistry of wolframite from the Baia Sprie epithermal deposit, Romania. Economic Geology, 97: 415–423.

Beuchat, S., Moritz, R., and Pettkeb, T., 2004. Fluid evolution in

the W-Cu-Zn-Pb San Cristobal vein, Peru: fluid inclusion and stable isotope evidence. Chemical Geology, 210: 201–224.
Campbell, A.R., Hackbarth, C.J., Plumlee, G.S., and Petersen, U., 1984. Internal features of ore minerals seen with the infrared microscope. Economic Geology, 79: 1387–1392.
Campbell, A.R., and Panter, K.S., 1990. Comparison of fluid inclusions in coexisting (cogenetic?) wolframite, cassiterite, and quartz from St. Michael's Mount and Cligga Head, Cornwall, England. Geochimica et Cosmochimica Acta, 54 (3): 673–681.
Campbell, A. R., and Robinson-Cook, S., 1987. Infrared fluid inclusion microthermometry on coexisting wolframite and quartz. Economic Geology, 82: 1640–1645.
Campbell, A.R., Robinson-Cook, S., and Amindyas, C., 1988. Observation of fluid inclusions in wolframite from Panasqueira. Portugal Bull. Mineral, 111: 252–256.
Cattalani, S., and Williams-Jones, A E., 1991. C-O-H-N fluid evolution at Saint-Robert, Quebec: Implications for W-Bi-Ag mineral deposition. Canadian Mineralogist, 29: 435–452.
Chen, T. H., 1982. On various features of the chemical composition of wolframites in a tungsten-tin deposit in Jiangxi province. Journal of Nanjing University (Natural Sciences), 1: 133–145 (in Chinese with English abstract).
Chi, G.X., and Lu, H.Z., 2008. Validation and representation of fluid inclusion assemblage (FIA)concept. Acta Petrol Sinica, 24(9): 1945–1953.
Clark, A. H., Kontak, D, J., and Farrar, E., 1990. The San Judas Tadeo W (-Mo, Au) deposit: Permian lithophile mineralization in southeastern Peru. Economic Geology, 85: 1651–1668.
Diamond, L.W. 1990. Fluid inclusion evidence for P-V-T-X evolution of hydrothermal solutions in late-Alpine gold-quartz veins at Brusson, Val D'Ayas, northwest Italian Alps. American Journal of Science, 290: 912–958
Giamello, M., Protano, G., Riccobono, F., and Sabaini, G., 1992. The W-Mo deposit of Perda Majori (SE Sardinia, Italy): a fluid inclusion study of ore and gangue minerals. European Journal of Mineralogy, 4: 1079–1084.
Goldstein, R.H., 2003. Petrographic analysis of fluid inclusions. In: Samson, I., Anderson, A., and Marshall, D. (eds.), Fluid Inclusions–Analysis and Interpretation. Mineralogical Association of Canada, Short Course Series, 32: 9–53.
Goldstein, R.H., and Reynolds, T.J., 1994. Systematics of fluid inclusions in diagenetic minerals. SEPM Short Course, 31: 1–199.
Graupner, T., Kempe, U., and Dombon, E., 1999. Fluid regime and ore formation in the tungsten (-yttrium) deposits of Kyzyltau (Mongolian Altai): Evidence for fluid variability in tungsten-tin ore systems. Chemical Geology, 154: 29–40.
Haapala, I., and Kinnunen, K., 1979. Fluid inclusions in Cassiterite and Beryl in Greisen Veins in the Eurajoki Stock, Southwestern Finland. Economic Geology, 74: 1231–1235.
Hagemann, S.G., and Lüders, V., 2003. P-T-X conditions of hydrothermal fluids and precipitation mechanism of stibnite-gold mineralization at the Wiluna lode-gold deposits, Western Australia: Conventional and infrared microthermometric constraints. Mineralium Deposita, 38: 936–952.
Hall, D.L., Sterner, S.M., and Bodnar, R.J., 1988. Freezing point depression of NaCl-KCl-H_2O solutions. Economic Geology, 83: 197–202.
He, Z.Y., Xu, X.S., Zou, H.B., Wang, X.D., and Yu, Y., 2010. Geochronology, petrogenesis and metallogeny of Piaotang granites in the tungsten deposit region of South China. Geochemical Journal, 44 (4): 299–313.
Heinrich, C.A., 1990. The chemistry of hydrothermal tin(-tungsten) ore deposition. Economic Geology, 85(3): 457–481.
Higgins, N. C., and Kerrich, R., 1982. Progressive ^{18}O depletion during CO_2 separation from a carbon dioxide-rich hydrothermal fluid: Evidence from the Grey River tungsten deposit, Newfoundland: Canadian Journal of Earth Sciences, 19: 2247–2257.
Hua, R.M., Zhang, W.L., Chen, P. R., and Wang, R.C., 2003. Comparison in the characteristics，origin and related metallogeny between granites in Dajishan and Piaotang, southern Jiangxi, China. Geological Journal of China Universities, 9(4): 609–619 (in Chinese with English abstract).
Hua, R.M., Zhang, W.L., Li, G.L., Hu, D.Q., and Wang, X.D., 2008. A preliminary study on the features and geologic implication of the Accompanying Metals in Tungsten Deposits in the Nanling Region. Geological Journal of Chinese Universities, 14(4): 527–538 (in Chinese with English abstract).
Huang, H.L., Chang, H.L., Tan, J., Li, F., Zhang, C.H., and Zhou, Y., 2015. Contrasting infrared microthermometry study of fluid inclusions in coexisting quartz, wolframite and other minerals: A case study of Xihuashan quartz-vein tungsten deposit, China. Acta Petrologica Sinica, 31(4): 925–940 (in Chinese with English abstract).
Jackson, N.J., Willis-Richards, J., Manning, D.A.C., and Sams, M.S., 1989. Evolution of the Cornubian ore field, Southwest England: Part II. Mineral deposits and ore-forming processes. Economic Geology, 84: 1101–1133.
Kelly, W.C., and Rye, R.O., 1979. Geologic fluid inclusion, and stable isotope studies of the tin-tungsten deposits of Panasqueira, Portual. Economic Geology, 74: 1721–1822.
Kouzmanov, K., Bailly, L., Ramboz, C., Rouer, O., and Beny. J.M., 2002. Morphology, origin and infrared microthermometry of fluid inclusions in pyrite from the Radka epithermal copper deposit, Srednogorie zone, Bulgaria. Mineralium Deposita, 37: 599–613.
Kouzmanov, K., Pettke, T., and Heinrich, C.A., 2010. Direct analysis of ore-precipitating fluids: Combined IR microscopy and LA-ICP-MS study of fluid inclusions in opaque ore minerals. Economic Geology, 105: 351–373.
Kucha, H., and Raith, J.G., 2009. Gold-oxysulphides in copper deposits of the Greywacke Zone, Austria: A mineral chemical and infrared fluid inclusion study. Ore Geology Reviews, 35: 87–100.
Landis, G.P., and Rye, R.O., 1974. Geologic, fluid inclusion and stable isotope studies of the Pasto Bueno tungsten base metal deposit, northern Peru. Economic Geology, 69: 1025–1059.
Lindaas, S.E., Kulis, J., and Campbell, A.R., 2002. Near-infrared observation and microthermometry of pyrite-hosted fluid inclusions. Economic Geology, 97: 603–618.
Little, W.M., 1960. Inclusions in cassiterite and associated minerals. Economic Geology, 55: 485–509.
Lu, H.Z., Fan, H.R., Ni, P., Ou, G.X., Shen, K., and Zhang, W.X., 2004. Fluid inclusion (First Edition). Beijing: Science Press, 1–487 (in Chinese).
Lüders, V., 1996. Contribution of infrared microscopy to fluid inclusion studies in some opaque minerals (wolframite, stibnite, bournonite): Metallogenic implications. Economic Geology, 91: 1462–1468.
Lüders, V., Gutzmer, J., and Beukes, N.J., 1999. Fluid inclusion studies in cogenetic hematite, hausmannite, and gangue minerals from high-grade manganese ores in the Kalahari manganese field, South Africa. Economic Geology, 94: 589–596.
Lüders, V., Romer, R.L., Cabral, A.R., Schmidt, C., and Banks, D.A., Schneider, J., 2005.Genesis of Itabirite-hosted Au–Pd–Pt-bearing hematite-(quartz) veins, Quadrilatero Ferrıfero, Minas Gerais, Brazil: Constraints from fluidinclusion infrared microthermometry, bulk crush-leach analysis and U-Pb systematics. Mineralium Deposita, 40: 289–306.
Lüders, V., and Ziemann, M., 1999. Possibilities and limits of infrared light microthermometry applied to studies of pyrite-hosted fluid inclusions. Chemical Geology, 154: 169–178.
Lynch, J.V.G., 1989. Hydrothermal alteration, veining, and fluid inclusion characteristics of the Kalzas wolframite deposit, Yukon. Canadian Journal of Earth Sciences, 26(10): 2106–2115.
Mancano, D.P., and Campbell, A.R., 1995. Microthermometry of enargitehosted fluid inclusions from the Lepanto, Philippines, high-sulfidation Cu-Au deposit. Geochimica et Cosmochimica Acta, 59: 3909–3916.
Moritz, R., 2006. Fluid salinities obtained by infrared microthermometry of opaque minerals: Implications for ore deposit modeling–A note of caution. Journal of Geochemical Exploration, 89: 284–287.
Mu, Z.G., Huang, F.S., Chen, C.Y., and Zheng, S.H., 1984.

Oxygen, hydrogen and carbon isotope studies of Piaotang and Xihuashan quartz vein-type tungsten deposits, Jiangxi province. In: Yu, H.Z. (ed.), Proceedings of Symposium on Tungsten Geology (Chinese Edition). Nanchang, 1981. Beijing: Geological Publishing House, 153–168 (in Chinese).

Nan, Y.Z., 1943. The tin deposits of southern Jiangxi (in Chinese). Geological Review, 8(Z1): 179–182.

Ni, P., Wang, X.D., Wang, G.G., Huang, J.B., Pan, J.Y., and Wang, T.G., 2015.An infrared microthermometric study of fluid inclusions in coexisting quartz and wolframite from Late Mesozoic tungsten deposits in the Gannan metallogenic belt, South China. Ore Geology Reviews, 65: 1062–1077

Ni, P., Li, W.S., and Pan, J.Y., 2020. Ore-forming fluid and metallogenic mechanism of wolframite-quartz vein-type tungsten deposits in South China. Acta Geologica Sinica (English Edition), 94(6): 1774–1796.

No. 932 Team of Nonferrous Metals Geological Exploration Company of Guangdong Province, 1966. How we use the 'five story' rule to find, evaluate and prospect quartz vein-type tungsten deposit. Geology and Prospecting, 5: 15–19 (in Chinese).

O'Reilly, C., Gallagher, V., and Feely, M., 1997. Fluid inclusion study of the Ballinglen W-Sn-sulphide mineralization, SE Ireland. Mineralium Deposita, 32: 569–580.

Polya, D.A., 1989. Chemistry of the main-stage ore-forming fluids of the Panasqueira W-Cu(Ag)-Sn deposit. Portugal: Implications for models of ore genesis. Economic Geology, 84: 1134–1152.

Polya, D.A., 1990. Pressure-dependence of wolframite solubility for hydrothermal vein formation. Transactions of the Institute of Mining and Metallurgy, 99: B120–B124.

Ramboz, C., Pichavant, M., and Weisbrod, A., 1982. Fluid immiscibility in natural processes: Use and misuse of fluid inclusion data. II. Chemical Geology, 37: 29–48.

Ramboz, C., Schnapper, D., and Dubessy, J., 1985. The P-V-T-X -fO_2 evolution of H_2O-CO_2-CH_4-bearing fluids in a wolframite vein: Reconstruction from fluid inclusion studies. Geochimica et Cosmochimica Acta, 49: 205–219.

Richards, J.P., and Kerrich, R., 1993. Observations of zoning and fluid inclusions in pyrite using a transmitted infrared light microscope ($\lambda < 1.9$ μm). Economic Geology, 88: 716–723.

Robinson-Cook, S.E., Campbell, A.R., Kyle, P.R., and Renault, J.R., 1986. An examination of the geochemical controls on transparency in wolframite (abs). Geological Society of America, 18(6): 731.

Roedder, E., 1984. Fluid inclusions. Mineralogical Society of America, Reviews in Mineralogy, 12: 644.

Samson, I.M., 1990. Fluid evolution and mineralization in a subvolcanic granite stock: The Mount Pleasant W-Mo-Sn deposits, New Brunswick, Canada. Economic Geology, 85: 145–163.

Seal, R.R.II., Clark, A.H., and Morrissey, C.J., 1987. Stockwork tungsten (scheelite)-molybdenum mineralization, Lake George, Southwestern New Brunswick. Economic Geology, 82: 1259–1282.

Shan, F., 1976. The geological characteristics of tungsten-tin deposits of a quartz-veinlets-zone type. Acta Geologica Sinica, (1): 1–16 (in Chinese with English abstract).

So, C.S., and Yun, S.T., 1994. Origin and evolution of W-Mo-producing fluids in a granitic hydrothermal system: Geochemical studies of quartz vein deposits around the Susan granite, Hwanggangri district, Republic of Korea. Economic Geology, 89: 246–267.

Su, W.C., Zhu, L.Y., Ge, X., Shen, N.P., Zhang, X.C., and Hu, R.Z., 2015. Infrared microthermometry of fluid inclusions in stibnite from the Dachang antimony deposit, Guizhou. Acta Petrologica Sinica, 31(4): 918–924 (in Chinese with English abstract)

Wang, X.D., Ni, P., Jiang, S.Y., Zhao, K.D., and Wang, T.G., 2010. Origin of ore-forming fluids of the Piaotang tungsten deposit in Jiangxi Province: Evidence from helium and argon isotopes. Chinese Science Bulletin, 55(7): 628–634.

Wang, X.D., Ni, P., Jiang, S.Y., Huang, J.B., and Sun, L.Q., 2008. Fluid inclusion study on the Piaotang tungsten deposit, southern Jiangxi Province, China. Acta Petrologica Sinica, 24 (9): 2163–2170 (in Chinese with English abstract).

Wang, X.D., Ni, P., Yuan, S.D., and Wu, S.H., 2013. Fluid inclusion studies on coexisting cassiterite and quartz from Piaotang Tungsten Deposit, Jiangxi Province, China. Acta Geologica Sinica, 87(6): 850–859 (in Chinese with English abstract).

Wei, W.F., Hu, R.Z., Bi, X.W., Peng, J.T., Su, W.C., Song, S.Q., and Shi, S.H., 2012. Infrared microthermometric and stable isotopic study of fluid inclusions in wolframite at the Xihuashan tungsten deposit, Jiangxi province. Mineralium Deposita, 47(7): 589–605.

Wood, S.A., and Samson, I.M., 2000. The hydrothermal geochemistry of tungsten in granitoid environments: I. Relative solubilities of ferberite and scheelite as a function of T, P, pH and mNaCl. Economic Geology, 95: 143–182.

Xu, J.X., Zeng, Z.L., Wang, D.H., Chen, Z.H., Liu, S.B., Wang, C.H., and Ying, L.J., 2008. A new type of Tungsten deposit in southern Jiangxi and the new model of 'Five Floors + Basement' for prospecting. Acta Geologica Sinica, 82(7): 880 –887 (in Chinese with English abstract).

Xu, K.Q., Hu, S.X., Sun, M.Z., Zhang, J.R., Ye, J., and Li, H., 1984a. Regional factors controlling the formation of tungsten deposits in south China. In: Yu, H.Z. (ed.). Proceedings of Symposium on Tungsten Geology (Chinese Edition). Nanchang, 1981. Beijing: Geological Publishing House, 245–249 (in Chinese).

Xu, K.Q., and Ding, Y., 1943. Geology of tungsten deposits in southern Jiangxi. Special Report of China Geological Survey, A17: 1–149 (in Chinese).

Xu, K.Q., Sun, N., Wang, D.Z., Hu, S.X., Liu, Y.J., and Ji, S.Y., 1984b. Genesis and metallogenesis of granites of South China. In: Xu, K.Q., and Tu, G.C. (eds.), Granite and Related of Metallogenesis (Collected Papers of international symposium). Nanjing: Jiangsu Science and Technology Press, 1–20 (in Chinese).

Yan, K.Y., 1944. The genesis of Piaotang tungsten-tin deposit, Dayu, southern Jiangxi. Geological Review, 9(Z1): 93–102 (in Chinese).

Zhang, J.Y., 1960. Preliminary study on properties of cassiterite of a certain tungsten-tin deposit in Dayu, Jiangxi province. Earth Science (Journal of China's University of Geosciences), 11: 8–11 (in Chinese).

Zhang, L.G., Zhuang, L.C., Qian, Y.Q., and Guo, Y.S., 1984. Stable isotope geochemistry of granites and tungsten-tin deposits in Xihuashan-Piaotang area, Jiangxi Province. In: Yu, H.Z. (ed.), Proceedings of Symposium on Tungsten Geology (Chinese Edition). Beijing: Geological Publishing House, 325 –338 (in Chinese).

Zhang, W.L., Hua, R.M., Wang, R.C., Li, H.M., Qu, W.J., and Ji, J.Q., 2009. New dating of the Piaotang granite and related Tungsten mineralization in Southern Jiangxi. Acta Geologica Sinica (English Edition), 83(5): 659–670.

Zhu, Y.L., Li, C.Y., and Lin, Y.H., 1981. Geology of tungsten deposit of southern Jixangxi Province. Nanchang: Jiangxi People's Publishing House, 1–419 (in Chinese).

About the first and corresponding author



WANG Xudong, male, born in 1975 in Shenyang, Liaoning Province; doctor; graduated from Nanjing University; lecturer at Yuanpei College of Shaoxing University. He is currently interested in geological fluids and mineralization. E-mail: wwwggd_009@163.com.